

Rhenium(I) complexes of readily functionalized bidentate pyridyl-1,2,3-triazole “click” ligands: A systematic synthetic, spectroscopic and computational study

Tae Y. Kim^a, Anastasia B.S. Elliott^{a,b}, Karl J. Shaffer^a, C. John McAdam^a, Keith C. Gordon^{a,b,*}, James D. Crowley^{a,*}

^a Department of Chemistry, University of Otago, P.O. Box 56, Dunedin, New Zealand

^b MacDiarmid Institute for Advanced Materials and Nanotechnology, New Zealand

ARTICLE INFO

Article history:

Available online 15 May 2012

This paper is dedicated to Alfred Werner on the 100th Anniversary of his Nobel prize in Chemistry in 1913.

Keywords:

“Click” chemistry
Rhenium
Emission lifetimes
Resonance Raman
Electrochemistry

ABSTRACT

A family of electronically tuned *fac*-Re(CO)₃Cl pyridyl-1,2,3-triazole complexes have been synthesized by refluxing methanol solutions of [Re(CO)₅Cl] and the substituted 2-(1-R-1H-1,2,3-triazol-4-yl)pyridine ligands (pytri-R). The resulting rhenium(I) complexes were characterised by elemental analysis, HR-ESMS, IR, ¹H and ¹³C NMR and in one case the molecular structure was confirmed by X-ray crystallography. The electronic structure of this family of *fac*-[(pytri-R)Re(CO)₃Cl] complexes was probed using UV-Vis, Raman and emission spectroscopy and cyclic voltammetry techniques. The complexes show intense absorptions in the visible region, comprising strong $\pi \rightarrow \pi^*$ and metal-to-ligand charge-transfer (MLCT) transitions, which were modelled using time-dependent density functional theory (TD-DFT). Interestingly, the MLCT transition energy and the emission maxima are unaffected by the nature of the R substituent on the 2-(1-R-1H-1,2,3-triazol-4-yl)pyridine ligand indicating that the 1,2,3-triazoyl unit is acting as an electronic insulator. The emission lifetimes of the complexes are modestly dependent on the nature of the 1,2,3-triazole substituent, with the conjugated complexes displaying longer lifetimes than the non-conjugated ones. The shorter lifetimes for complexes with non-conjugated ligands are attributed to the “free-rotor” effect which allows molecules to relax through non-radiative pathways. In this case, the freely rotating CH₂ group located between the triazole and the R group causes the decrease in excited lifetime. The electrochemistry of all examples is defined by irreversible Re oxidation and triazole based ligand reduction processes. The nitro substituted complexes show additional nitrobenzene type reduction features. Similarly, the ferrocenyl substituted complex displays the expected reversible one electron oxidation process. Consistent with the spectroscopic data, the position of the oxidation and reduction processes are essentially unaffected by the electronic nature of the 2-(1-R-1H-1,2,3-triazol-4-yl)pyridine substituent.

© 2012 Elsevier Ltd. All rights reserved.

1. Introduction

Rhenium was not officially known when Alfred Werner was awarded his Nobel Prize in 1913. In the intervening century the element rhenium was discovered and the coordination chemistry for Re^I was developed. Complexes of rhenium are extensively used in catalysis [1,2] and recently there has been considerable interest in *fac*-[(α -diimine)Re(CO)₃Cl] complexes, especially those containing 2,2'-bipyridine (bpy) and 1,10-phenanthroline, as they have been shown to have interesting photophysical properties [3–5]. These *fac*-[(α -diimine)Re(CO)₃Cl] complexes have been exploited as photocatalysts for the reduction of CO₂ [6], as sensors [5,7,8] and as bioimaging agents [9,10]. The 2-(1-R-1H-1,2,3-triazol-4-

yl)pyridine (pytri-R) family of ligands have recently emerged as tunable 2,2'-bipyridyl analogues [11–13], because they can be readily synthesized using the Cu^I-catalyzed 1,3-cycloaddition of organic azides with terminal alkynes (the CuAAC reaction) [14–18]. Complexes with Ag^I [19–21], Cu^I [21], Cu^{II} [19,22,23], Pd^{II} [24–27], Pt^{II} [24], Zn^{II} [28], Pb^{II} [29], Ru^{II} [30–34], and Ir^{III} [34–38] have been synthesized and structurally characterized.

A number of these studies have examined electronic structure and photophysical properties of the 2-(1-R-1H-1,2,3-triazol-4-yl)pyridine complexes. Many of these studies have focused on the effect of the triazole N1-substituent on the properties of the complex. Felici et al. [34] reported the emission properties of complexes of [Ir(ppy)₂(pytri-R)]⁺ where the triazole–pyridine ligand contained either adamantyl or cyclodextrin (CD) substituents. The emission from these compounds originated from the Ir(ppy) luminophore. The complex with the CD-substituent showed a very high quantum yield for emission; which was attributed to the protection afforded to the complex by this bulky group. In a detailed

* Corresponding authors. Tel.: +64 3 4797731; fax: +64 3 4797906 (J.D. Crowley).

E-mail addresses: Kgordon@chemistry.otago.ac.nz (K.C. Gordon), jcrowley@chemistry.otago.ac.nz (J.D. Crowley).

study of $[\text{Ir}(\text{F}_2\text{ppy})_2(\text{pytri-R})]^+$ complexes (where F_2ppy is difluorophenyl-pyridine based and pytri-R is N1 substituted with adamantyl, benzyl, biphenyl and phenyl substituents) Mydlak et al. [38] show that emission for each of these complexes is predominantly $\text{Ir}(\text{F}_2\text{ppy})$ based. The triazole substituent however does have an effect on the photophysics of the complex. It is noted that the emission lifetime for the biphenyl substituted complex is almost three times longer than for the other complexes. This is attributed to the lowering in energy of the π^* MO on the pytri-R ligand that results in greater mixing of states and an increase in the ^3LC character of the lowest excited state and thus an increased lifetime. It was possible to use these compounds in the fabrication of OLEDs with very blue emission properties. Liu et al. [37] report the photophysics of $[\text{Ir}(\text{ppy})_2(\text{pytri-R})]^+$ and $[\text{Ir}(\text{F}_2\text{ppy})_2(\text{pytri-R})]^+$ complexes with R being fluoroalkyl, fluorophenyl and fluorotolyl substituents. The photophysical properties reveal emissive states of $\text{Ir}(\text{ppy})$ nature. Happ et al. [32] showed that for ruthenium(II) complexes with 4,4'-dimethyl-2,2'-bipyridine (dmbpy) and pytri-R ligands, of the form $[\text{Ru}(\text{dmbpy})_3-n(\text{pytri-R})_n]^{2+}$, emission occurs from the dmbpy Ru^3MLCT chromophore unless $n = 3$, when emission from the Ru pyridyl-1,2,3-triazole $^3\text{MLCT}$ is blue-shifted by up to 29 nm in *n*-butyronitrile glass at 77 K. These studies provide evidence that the pyridyl-1,2,3-triazole and the substituents borne on the N1 position can affect the electronic structure and emission properties of complexes. A more direct way to probe this interaction is to study emissive complexes in which the chromophore and luminophore are metal (pyridyl-1,2,3-triazole) based. This may be explored using $[\text{Re}(\text{CO})_3\text{Cl}]$ as a binding unit. In the case of $[(\text{pytri-R})\text{Re}(\text{CO})_3\text{Cl}]$ complexes several studies have been conducted. Obata et al. [39] synthesized $[(\text{pytri-R})\text{Re}(\text{CO})_3\text{Cl}]$ where R = benzyl or a sugar unit. They studied the electronic structure of these systems using DFT and electronic absorption and emission spectroscopic methods. The TD-DFT calculations reveal that the $\text{HOMO} \rightarrow \text{LUMO}$ transition was MLCT in nature and was well modelled. This predicted that the MLCT transition would be to the blue of the $\text{Re} \rightarrow \text{bpy}$ MLCT, which is observed. The emission from $\text{Re} \rightarrow \text{pytri-R}^3\text{MLCT}$ (where R = benzyl) was also blue-shifted (at 538 nm in CH_3CN) compared to the $\text{Re}(\text{bpy})$ luminophore (which lies at 633 nm).

The ability of pytri-R to facilitate electronic communication between differing emitting centres has been investigated in an elegant systematic fashion by Rowan et al. [36] In this study $[\text{Ir}(\text{ppy})_2]$ and $\text{Ir}(\text{C}^*\text{N}')_2$ (where $\text{C}^*\text{N}'$ is 1-phenylpyrazole) units were bound to pytri-R and these ligands in turn were connected via the (N1) sp^2 triazole nitrogen to form dimer and trimer structures. This study found that the photophysical properties of the individual Ir units were unperturbed by the modulation of linker groups through the N1 sp^2 triazole nitrogen. Gratzel et al. [40] have shown that an analogue to the N719 dye [41] (used in dye-sensitised solar cells) with pytri-R ligand $[\text{Ru}(\text{pytri-R})(\text{bpy}(\text{CO}_2\text{H})_2)(\text{CNS})_2]$ provides a cell with 7% efficiency. This is impressive in view of the poor spectral coverage the pytri-R dye affords in comparison to N719. In a DFT analysis it is shown that the LUMO and LUMO+1 of $[\text{Ru}(\text{pytri-R})(\text{bpy}(\text{CO}_2\text{H})_2)(\text{CNS})_2]$ are based on the bpy ligand. Happ et al. [42] have carried out a systematic study of substituent effects on the ruthenium complexes with a substituted pytri-R ligand $[\text{Ru}(\text{dmbpy})_2(\text{pytri-R})]^{2+}$. Substitution with ethynyl phenyl groups occurs at either the 5-pyridyl or N1 triazole positions. Substitution of the 5-pyridyl position has a striking effect on the emission properties – tuning the emission wavelength from 602 nm with 1-ethynyl-4-methoxybenzene to 674 nm with 1-ethynyl-4-nitrobenzene. However the 1-ethynyl-4-nitrobenzene substituted at the N1 triazole nitrogen results in an emission at 610 nm – effectively the potent electron withdrawing power of this substituent is insulated from the Ru centre by linkage through the triazole.

Ruthenium complexes with the DNA active moiety $[\text{Ru}(\text{TAP})_2(\text{pytri-R})]^{2+}$ (where TAP = 1,4,5,8 tetraazaphenanthracene) have also been reported [43]. The most notable effect of pytri-R ligand is that the Ru $d\pi$ orbitals are stabilised by ~ 50 mV relative to L = 1,10-phenanthroline; presumably a consequence of poorer overlap between the $d\pi$ and $\pi^*(\text{pytri-R})$ MOs.

In a study of pytri-OBu it was found that presence of alkaline and selected first row transition metals resulted in varying levels of emission intensity but no tuning of the emission which was observed at 500 nm [44].

Altering the N1 substituent does not appear to radically shift the emission spectrum for $[(\text{pytri-R})\text{Re}(\text{CO})_3\text{Cl}]$ complexes. For example the emission maxima for substituted $[(\text{pytri-R})\text{Re}(\text{CO})_3\text{Cl}]$ (where R = $(\text{CH}_2)_2\text{CO}_2\text{H}$) lies at 526 nm in DMF/MeOH [45] and with R = (2-methoxyphenyl)piperazine it is reported at 522 nm (in MeOH) [46]. It is notable that the DFT calculations conducted on these systems show modest contribution from the N1 substituent in the LUMOs.

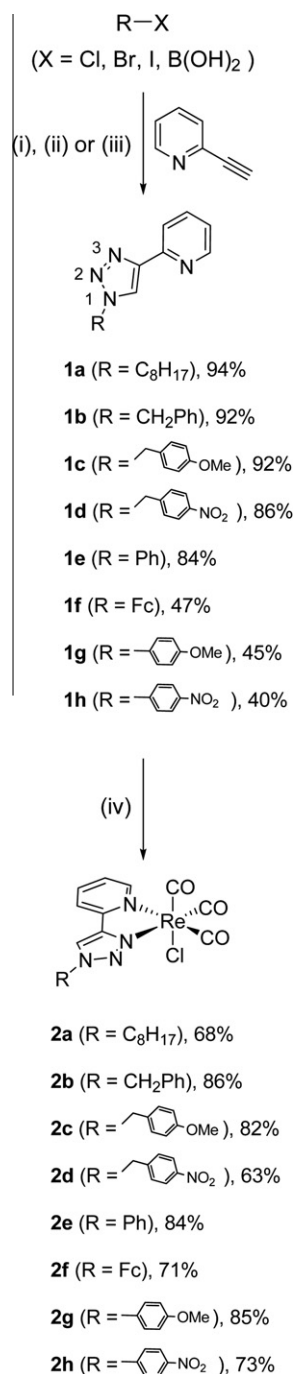
Herein we extended the work of Obata [39] and Benoist [45,46] and generate a family of electronically tuned *fac*- $\text{Re}(\text{CO})_3\text{Cl}$ 2-(1-R-1H-1,2,3-triazol-4-yl)pyridine complexes. Efficient safe one-pot CuAAC “click” methodologies were exploited to synthesize a series of electronically modified 2-pyridyl-1,2,3-triazole ligand architectures which were readily converted into the corresponding family of *fac*- $[\text{Re}(\text{CO})_3\text{Cl}]$ complexes. In this systematic study the electronic structure of a series of *fac*- $[(\text{pytri-R})\text{Re}(\text{CO})_3\text{Cl}]$ complexes in which the substituents are capable of conjugative coupling with the triazole and insulated via a CH_2 group from such communication are examined. In order to probe the nature of the lowest energy transition resonance Raman spectroscopy was utilised in concert with DFT calculations. The nature of the lowest excited state was established using time-resolved emission spectroscopy.

2. Results and discussion

2.1. Ligand synthesis and characterization

We have previously used efficient one-pot CuAAC “click” methodologies to synthesize a range of substituted 2-(1-R-1H-1,2,3-triazol-4-yl)pyridine (**1a**, **1b**, **1e** and **1f**) ligands [19,20,24,25]. The same methodologies were exploited to generate a family of electronically tuned 2-pyridyl-1,2,3-triazole ligand architectures (Scheme 1). We have described [19,24,25] the synthesis of the 2-pyridyl-1,2,3-triazole ligands **1a** (R = octyl) and **1b** (R = Bn) using standard Fokin [47] conditions and found the same methodology could be applied to the synthesis of the electronically modified benzyl substituted ligands, **1c** (R = 4-methoxybenzyl) and **1d** (R = 4-nitrobenzyl). Simply mixing 2-ethynylpyridine, the appropriate benzyl bromide/chloride, NaN_3 , $\text{CuSO}_4 \cdot 5\text{H}_2\text{O}$, Na_2CO_3 and L-ascorbic acid in DMF/ H_2O (4:1) then stirring at room temperature (**1c** and **1d**) for 20 h provided, after a simple work up, the desired ligands (86–92%, Scheme 1(i)) without the need for isolating the potentially hazardous azide intermediates.

The methods of Liang [48,49] and Guo/Aldrich [50,51] have previously been applied for the synthesis of the aryl substituted 2-(1-R-1H-1,2,3-triazol-4-yl)pyridine (**1g** and **1h**) ligands. As 4-iodoanisole is commercially available we elected to use the conditions of Liang and co-workers [48,49] to generate the 4-methoxyphenyl substituted ligand **1g**. A mixture of 4-iodoanisole, NaN_3 , sodium L-ascorbate, *N,N'*-dimethylethylenediamine and CuI, were heated at 100 °C for 1.5 h in EtOH/ H_2O (2:1) to generate the arylazide intermediate *in situ* (Scheme 1(ii)). The reaction mixture was cooled to room temperature, 2-ethynylpyridine, $\text{CuSO}_4 \cdot 5\text{H}_2\text{O}$, and sodium L-ascorbate were added and the Cu^I-catalysed 1,3-cycloaddition reaction proceeded at room temperature over 16 h



Scheme 1. (i) NaN₃, CuSO₄·5H₂O, ascorbic acid, Na₂CO₃, DMF/H₂O (4:1), RT or 95 °C, 20 h; (ii) (a) NaN₃, sodium L-ascorbate, N,N'-dimethylethylenediamine, CuI, 100 °C, 1.5 h, (b) CuSO₄·5H₂O, sodium L-ascorbate; (iii) (a) NaN₃, Cu(OAc)₂, MeOH, 55 °C, 2 h, (b) sodium L-ascorbate, RT, 16 h; (iv) [Re(CO)₅Cl], 70 °C, 6 h or 20 h.

to give **1g** in modest yield (45%). The method of Aldrich [50] was exploited to convert 4-nitrophenylboronic acid into the nitrophenyl substituted ligand **1h** (Scheme 1(iii)). Stirring 4-nitrophenylboronic acid, NaN₃, and Cu(OAc)₂ in dry MeOH for 2 h at 55 °C resulted in the *in situ* generation of the azido intermediate. After cooling to room temperature, sodium L-ascorbate and 2-ethynylpyridine were added and the resulting suspension was stirred at room temperature for a further 16 h, yielding the desired ligand **1h** in modest yield (40%), but without the need for isolating the potentially hazardous azide intermediate. The yield of **1h** (40%) was depressed relative to **1e** (84%). The corresponding 4-nitrophenyl

nylazide had been shown to form in high yield (85%) [50] so the problem appeared to be during the Cu^I-catalysed 1,3-cycloaddition step. This could potentially be due to the electron withdrawing nitro group deactivating the azide. Alternatively, the low yield could be connected the instability of nitro substituted arylazide as has been observed before [52].

The new ligands (**1c** and **1d**) and the known ligands synthesized using *in situ* methodologies (**1g** and **1h**) have been characterized by elemental analysis, HR-ESMS, IR, ¹H and ¹³C NMR spectroscopy. For example, the diagnostic singlet, in the ¹H NMR spectra of the ligands, corresponding to the triazole unit was found between 8.7 and 8.4 ppm (see Supporting Information).

2.2. Synthesis of Re(I) complexes

Obata [39] and Benoist [45,46] have independently synthesized a series of *fac*-[Re(CO)₃Cl] complexes of substituted 2-(1-R-1H-1,2,3-triazol-4-yl)pyridines [R = Bn (**2b**), COOCH₃, COOH, CH₂CH₂-glucose, and CH₂CH₂-(2-methoxyphenyl)piperazine] by simply refluxing methanol solutions of [Re(CO)₅Cl] and the substituted 2-(1-R-1H-1,2,3-triazol-4-yl)pyridine ligands. Exploiting the same methodology we generated the family of electronically tuned rhenium(I) complexes (**2a–h**). One of the ligands (**1a–h**, 1 equiv) was added to a methanol solution of [Re(CO)₅Cl] (1 equiv) and the resulting reaction mixture was heated at reflux for 6–20 h (Scheme 1). This provided complexes (**2a–h**) in good to excellent yields (63–86%) [39,45,46]. The rhenium(I) compounds have been characterized by elemental analysis, HR-ESMS, IR, ¹H and ¹³C NMR spectroscopy. Elemental analysis confirmed that the isolated powders were pure and indicated that the bidentate “click” ligands (**1a–h**) formed rhenium(I) complexes with a 1:1 metal/ligand ratio. Consistently, the HR-ESMS spectra (dissolution in DMSO followed by methanol elution) showed the presence of the neutral complexes ionised as Na⁺ adducts (*fac*-[(pytri-R)Re(CO)₃Cl](Na)⁺). ¹H NMR spectra of the rhenium(I) complexes were recorded at room temperature in d₆-DMSO (see Supporting Information) and when compared with the spectra of the corresponding ligands, the pyridyl and triazole proton signals of the complexes were shifted downfield indicative of metal complexation (Fig. S1 in Supporting Information). Three strong ν(CO) stretching bands are observed in the region of 2029–1882 cm⁻¹, indicative of the presence of the *fac*-[Re(CO)₃Cl] core [39,45,46]. Unequivocal proof of this facial (*fac*) coordination geometry was obtained from X-ray crystallography (*vide infra*).

The X-ray crystal structure of **2c** was obtained using single crystals grown by vapour diffusion of diethyl ether into an acetonitrile solution of the complex. The complex crystallised in the triclinic space group and showed the expected coordination geometry about the rhenium(I) centre (Fig. 1, Table S1 in Supporting Information). The bond lengths and angles for **2c** are similar to those previously observed for **2b** [39] (Table S2 in Supporting Information).

2.3. Electronic structure

The electronic structure of the *fac*-[(pytri-R)Re(CO)₃Cl] complexes was investigated using both computational and spectroscopic methods. The veracity of computational methods may be ascertained by comparison of calculated parameters with experimental data. We have used X-ray crystallographic data, where available, to compare to the calculated structures and FT-Raman spectra compared to simulated spectra obtained through frequency calculations.

DFT calculations of a number of bond lengths and angles are compared to experimental values for **2c** in Table 1. They show that DFT models the molecular geometry with all but one bond length differing by <0.0024 Å and angles by <3°.

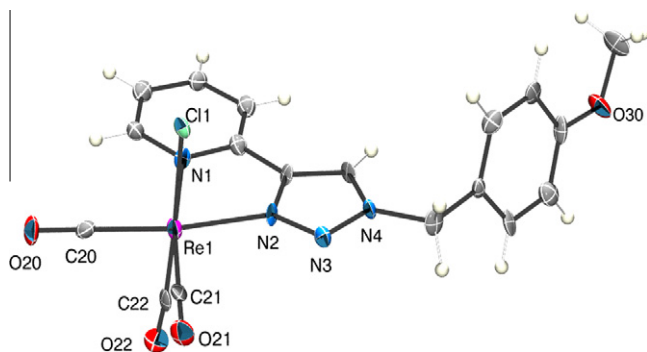


Fig. 1. ORTEP drawing of **2c** with thermal ellipsoids shown at 50% probability. Selected bond lengths (Å) and angles (°) for **2c**: N1–Re1 2.2002 (54), N2–Re1 2.1557 (54), C11–Re1 2.5051 (18), C22–Re1 1.9271 (87), C21–Re1 1.9236 (74), C20–Re1 1.9141 (73); N1–Re1–N2 73.88 (20), N1–Re1–C11 84.98 (16), N2–Re1–C22 96.37 (25), C22–Re1–C11 176.49 (21), C20–Re1–C21 89.39 (29), C21–Re1–C22 88.67 (29).

Table 1

Comparison of bond lengths (Å) and angles (°) for **2c** obtained from X-ray crystal structure data and DFT calculations using the B3LYP method and LANL2DZ basis set for Re and the 6-31g(d) basis set for the remaining molecules. Numbering is given in Fig. 1.

| Bond/angle | X-ray | Calculation |
|-------------|-------------|-------------|
| N1–Re1 | 2.2002 (54) | 2.24 |
| N2–Re1 | 2.1557 (54) | 2.18 |
| C11–Re1 | 2.5051 (18) | 2.53 |
| C22–Re1 | 1.9271 (87) | 1.92 |
| C21–Re1 | 1.9236 (74) | 1.93 |
| C20–Re1 | 1.9141 (73) | 1.93 |
| N1–Re1–N2 | 73.88 (20) | 74.1 |
| N1–Re1–C11 | 84.98 (16) | 82.6 |
| N2–Re1–C22 | 96.37 (25) | 94.2 |
| C22–Re1–C11 | 176.49 (21) | 175.5 |
| C20–Re1–C21 | 89.39 (29) | 90.8 |
| C21–Re1–C22 | 88.67 (29) | 91.7 |

In comparing the Raman spectra (simulated and experimental) we have used the mean absolute deviation (MAD) of wavenumbers, for bands between 400 and 1650 cm^{-1} that have greater than 20% maximum band intensity.¹ A typical comparison is shown in Fig. 2. For these systems MADs of <10 cm^{-1} are obtained; this is considered to give a useful model of the electronic structure of the complex of interest [53–65].

Electronic absorption spectra of **2a–h** are shown in Fig. 3. The spectra show a lowest energy transition at approximately 330 nm that is unaffected by substitution whether it be unconjugated with the triazole ring (**2a–d**) or conjugated (**2e–h**).

The band at 330 nm is assigned to a metal–ligand charge-transfer (MLCT) based on previous literature assignments [39]. Furthermore this assignment is supported by the TD-DFT data which is summarised in Table 2. At shorter wavelengths there are additional transitions associated with the ligand (275 nm) and higher energy MLCT transitions (290 nm).

The TD-DFT data predict that the lowest energy transition in the complexes with non-conjugated substituents (**2a–d**) is MLCT in nature and is unshifted in energy through the series (predicted at 358, observed at 330 nm) – this is what is observed. In the case of the complexes with conjugated substituents on the triazole (**2e–h**) shifts are predicted and these are not observed in the experimental data. One reason for this discrepancy between calculated

¹ The carbonyl bands are not used in this MAD comparison as they are more anharmonic than the skeletal modes in the 300–1650 cm^{-1} region [56]; for this reason they require a differing scaling factor and as there are only three bands they are not included.

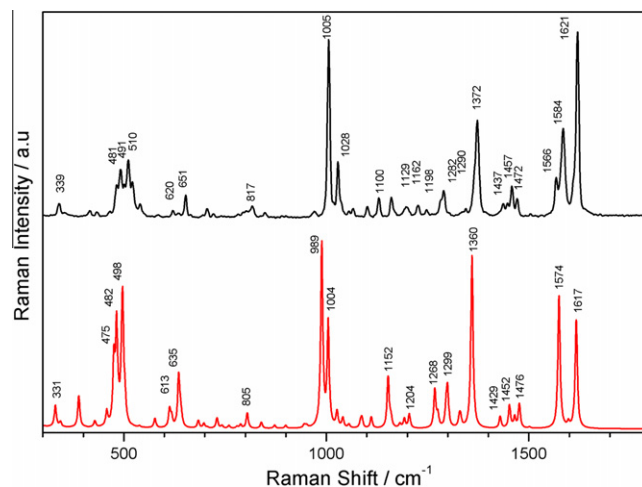


Fig. 2. Comparison of experimental (upper, black trace) FT-Raman spectrum of **2b** with the simulated spectrum (lower, red trace). (Colour online.)

and observed spectral behaviour is that density functional theory systematically overestimates conjugative effects. Thus, in this case the effect of the conjugated group is predicted to be stronger than observed [66]. It should be noted that TD-DFT calculations are often shifted compared to experimental observation by up to 0.4 eV [67].

The nature of the MLCT band at 330 nm differs subtly between the complexes with conjugated and non-conjugated ligands. In all cases the donor orbital is Re $d\pi$ in nature. The acceptor orbital however differs in a systematic way; for the unconjugated complexes (**2a–d**) it is localised solely on the triazole unit while the conjugated complexes display an MO that is spread over the R substituent in addition to the triazole moiety (Fig. 4). Some of this difference is a consequence of the overweighting of the conjugation interactions associated with the DFT method, this may be tested experimentally by measuring the resonance Raman spectroscopy.

Resonance Raman spectroscopy may be used to probe the nature of electronic transitions, this is because the resonance effect causes an enhancement of bands that reflect the structural changes

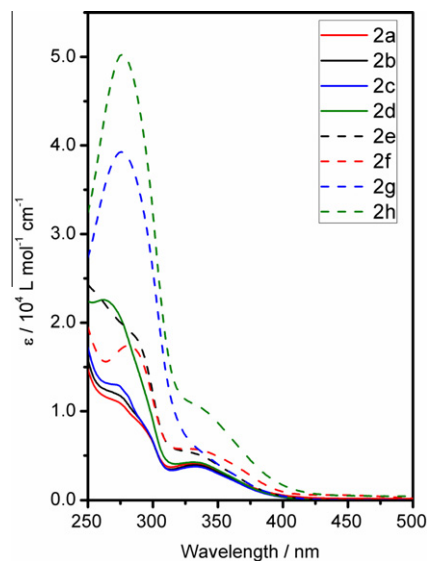


Fig. 3. Electronic absorption spectra of complexes obtained at 10^{-5} M in CH_3CN . Unconjugated molecules (**2a–d**) are shown as solid traces while conjugated ones are dashed (**2e–h**).

Table 2
Comparison of experimental electronic absorption data (from Fig. 3) with calculated TD-DFT data for **2a–h**.

| Complex | Experimental | | Calculated | | |
|-----------|----------------|--|----------------|--------|--|
| | λ (nm) | ϵ (L M ⁻¹ cm ⁻¹) | λ (nm) | f | Configuration (coefficient) |
| 2a | 333 | 11 600 | 358 | 0.070 | H-1 → LUMO (0.98) |
| | 288 | 9400 | 280 | 0.017 | HOMO → L+2 (0.28) HOMO → L+4 (0.52) |
| | 273 | 4100 | 273 | 0.18 | H-3 → LUMO (0.67) |
| 2b | 336 | 12 300 | 358 | 0.070 | H-1 → LUMO (0.97) |
| | 290 | 9500 | 296 | 0.015 | HOMO → L+1 (-0.12), HOMO → L+2 (0.50), HOMO → L+3 (-0.14) |
| | 270 | 3800 | 272 | 0.20 | H-5 → LUMO (0.66) |
| 2c | 333 | 3900 | 358 | 0.072 | H-2 → LUMO (0.64), H-1 → LUMO (-0.34) |
| | 290 | 9500 | 282 | 0.030 | H-2 → L+1 (-0.13), H-1 → L+1 (-0.20), HOMO → L+2 (0.19), HOMO → L+4 (0.25) |
| | 272 | 13 000 | 272 | 0.19 | H-5 → LUMO (0.66) |
| 2d | 333 | 4200 | 358 | 0.065 | H-1 → L+1 (0.95) |
| | 292 | 12 700 | 294 | 0.024 | H-1 → L+2 (0.45), H-1 → L+3 (0.12), H-1 → L+4 (-0.16) |
| | 265 | 22 600 | 279 | 0.22 | H-6 → LUMO (-0.26), H-4 → LUMO (0.68) |
| 2e | 330 | 5500 | 317 | 0.055 | H-1 → L+1 (0.94) |
| | 278 | 19 700 | 284 | 0.14 | H-3 → LUMO (0.71), H-1 → L+2 (-0.17) |
| 2f | 330 | 5600 | 307 | 0.06 | H-3 → L+1 (0.90) |
| | 282 | 17 300 | 272 | 0.160 | H-7 → LUMO (0.57), H-5 → L+1 (-0.27) |
| 2g | 330 | 6500 | 309 | 0.127 | H-1 → L+1 (0.87) |
| | 277 | 39 300 | 288 | 0.460 | H-2 → L+1 (0.86) |
| 2h | 330 | 11 000 | 363 | 0.0641 | H-2 → LUMO (0.20), H-1 → L+1 (0.77) |
| | 277 | 50 300 | 277 | 0.2659 | H-3 → L+1 (0.74) |

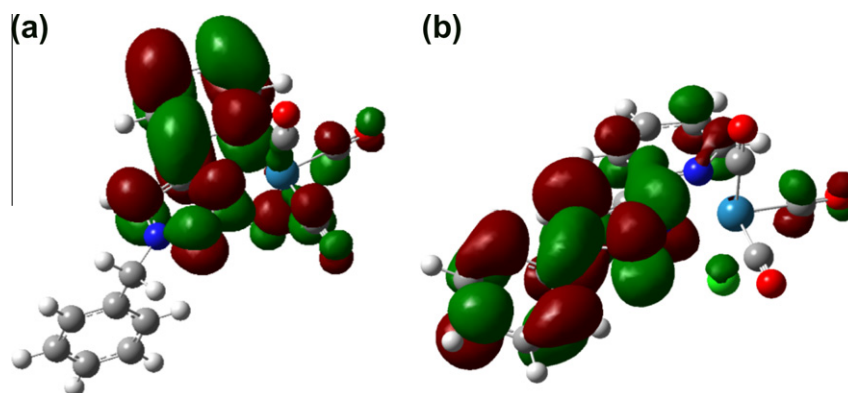


Fig. 4. Molecular orbital pictures of the main acceptor orbitals of **2b** (a) and **2e** (b) obtained from theoretical calculations.

that are associated with the photoexcitation [62,63,65,68–70]. Thus the pattern of band enhancements, coupled with knowledge of the nature of the normal modes of vibration which is obtained from the frequency calculations, can provide an insight into the structural nature of the donor and acceptor MOs [71]. The normal Raman spectra for the compounds are shown in Fig. 5. The spectra differ as the complexes have different substitution on the triazole ring; for example the spectra of **2d** and **2h** both show a distinctive band at 1349 cm⁻¹ associated with the NO₂ functionality [72,73].

The resonance Raman spectra are shown in Fig. 6. A striking feature of these data is the similarity between the spectra for the complexes **2a–d** which all show bands at 1285, 1571, 1587 and 1625 cm⁻¹; indeed these spectra appear almost identical. The frequency calculations provide normal modes for these bands; these are based on the pytri moiety (Fig. 7(a)). For the conjugated systems, **2e–h** small spectral differences are observed. In the case of **2e** the pytri modes observed in the non-conjugated systems are present; in addition there are weak bands at 1508 and 1601 cm⁻¹ which are due to modes that involve stretching of the

phenyl R group as well as the pytri. In the spectra of **2f** and **2g** the lower frequency mode attributed to stretching of the R-triazole moiety shifts to 1515 and 1522 cm⁻¹ – consistent with a mode that involves the conjugated aryl group. The spectrum of **2h** shows enhancement of the NO₂ group at 1349 cm⁻¹ [72,73] consistent with an acceptor MO that has some nitro character and thus involves the group appended to the triazole.

2.4. Excited state spectroscopy

The emission data for the complexes **2a–2h** are presented in Table 3. These data show that the R group substitution has no effect on the emission spectral profile; the lifetimes however are altered by these substituents. It is interesting to note that the nitro substituted compounds also show cyclic voltammetry traces that differ dramatically from those of the other compounds (*vide infra*).

The emission spectra of Re complexes of the type [(pytri-R)Re(-CO)₃Cl], with R = COOMe or CO^tBu, show maxima at 526 nm, while [(bpy)Re(CO)₃Cl] has an emission band at 598 nm [45].

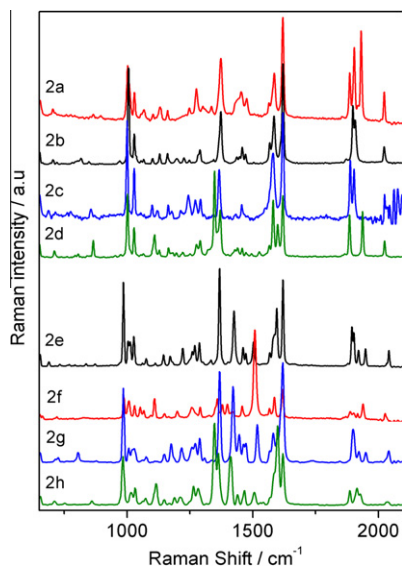


Fig. 5. FT-Raman spectra of the complexes **2a–h** obtained as solid samples at 1064 nm.

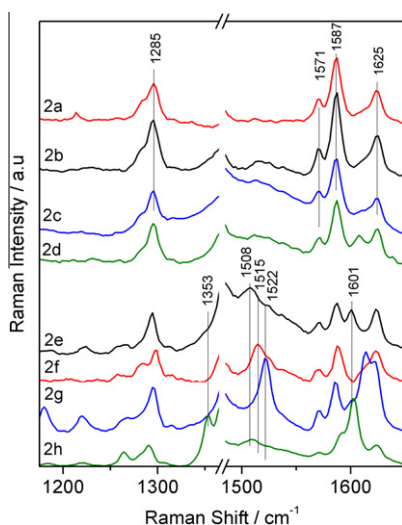


Fig. 6. Resonance Raman spectra of complexes **2a–h** obtained in CH₃CN at 10^{−3} M concentrations using 350.7 nm excitation. The spectral region between 1370 and 1490 cm^{−1} is dominated by strong solvent bands and has been omitted for clarity.

Lifetimes vary around 100 ns with those of the conjugated complexes, **2e–f** and **2h**, being longer than the non-conjugated ones,

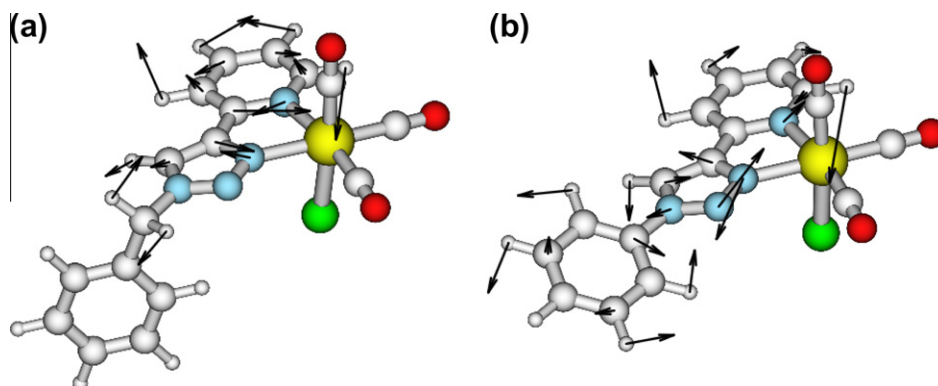


Fig. 7. The vibrational mode of **2b** at 1282 cm^{−1} (a) and **2e** at 1288 cm^{−1} (b) obtained from quantum calculations.

Table 3

Emission maxima, obtained in CH₃CN at 364 nm excitation, and emission lifetimes, obtained in CH₃CN at 354.7 nm, of **2a–h** at room temperature.

| Complex | λ_{em} (nm) | τ_{em} (ns) | $\Phi \times 10^{-2}$ | $k_r \times 10^5$ (s ^{−1}) | $k_{nr} \times 10^6$ |
|-----------|---------------------|------------------|-----------------------|--------------------------------------|----------------------|
| 2a | 532 | 121 ^a | 1.2 ^a | 1.0 ^b | 8.2 ^b |
| 2b | 532 | 103 | 1.2 | 1.2 | 9.6 |
| 2c | 533 | 79 | 1.3 | 1.7 | 12.4 |
| 2d | 532 | 7 | 0.1 | 1.5 | 143 |
| 2e | 532 | 162 | 3.6 | 2.2 | 6.0 |
| 2f | No emission | – | | | |
| 2g | 533 | 127 | 1.5 | 1.2 | 7.8 |
| 2h | 532 | 61 | | | |

^a ±10%.

^b ±20%.

2a–d. For example **2b** and **2c** have lifetimes of 103 and 79 ns, respectively, compared to their conjugate analogues **2e** and **2g** of 162 and 127 ns. Comparatively, the lifetimes of **2d** and **2h** (R = 4-NO₂Bn and 4-NO₂Ph) also show this trend but with considerably shorter lifetimes. Previously, the lifetime of [(bpy)Re(CO)₃Cl] and **2b** was measured by Obata et al. [39] in 2-methyltetrahydrofuran at 77 K as 3170 and 8900 ns, respectively. The shorter lifetime for complexes with non-conjugated ligands may be due to the “free-rotor” effect [74] which allows molecules to relax through non-radiative pathways. In this case, the freely rotating CH₂ group that connects the triazole and the R group causes the decrease in excited lifetime.

2.5. Cyclic voltammetry

Many electrochemical studies have been performed on rhenium tricarbonyl(α -diimine)chloride complexes [75,76]. Such systems are characterized by an irreversible Re^I/Re^{II} oxidation that occurs near the solvent limit, and ligand based reductions. As might be expected, the large variation in diimine ligand type (and substituents they carry) is mirrored in an equally diverse reduction chemistry, with multiple electron processes of variable reversibility, and halide exchange reactions commonly encountered.

The electrochemistry of ligands **1b**, **1e** [27] and **1f** [24] have previously been described. 1,2,3-triazoles typically undergo an irreversible reduction at very high negative potentials near the solvent limit [26,27]. Coordination to Pd or Pt shifts E_{pc} of the ligand reduction to less negative potential, but the process remains irreversible [24,26,27].

The electrochemistry of the rhenium compounds **2a–h** in CH₂Cl₂ solution was probed using cyclic voltammetry and Bu₄NPF₆ as supporting electrolyte. Data are presented in Table 4 and representative voltammograms for **2b**, **2f** and **2h** in Fig. 8. An internal

Table 4

Electrochemical data for **2a–h** (1×10^{-3} M in CH_2Cl_2 solution, 0.1 M Bu_4NPF_6 , referenced with internal $[\text{Fc}^{+}/0]$).

| Compound | E_{pc} (V) (triazole) | E_{pc} (V) (nitrobenzene) | E° (V) (nitrobenzene) | E° (V) (ferrocenyl) | E_{pa} (V) (Re^{I}) |
|-----------|-----------------------------------|---------------------------------------|---------------------------------|-------------------------------|---|
| 2a | -1.74 | | | | 1.49 |
| 2b | -1.72 | | | | 1.50 |
| 2c | -1.72 | | | | 1.49 |
| 2d | | -1.53 | -0.94 | | 1.50 |
| 2e | -1.66 | | | | 1.50 |
| 2f | -1.71 | | | 0.85 | 1.52 |
| 2g | -1.68 | | | | 1.50 |
| 2h | -1.73 | -1.31 | -0.81 | | 1.53 |

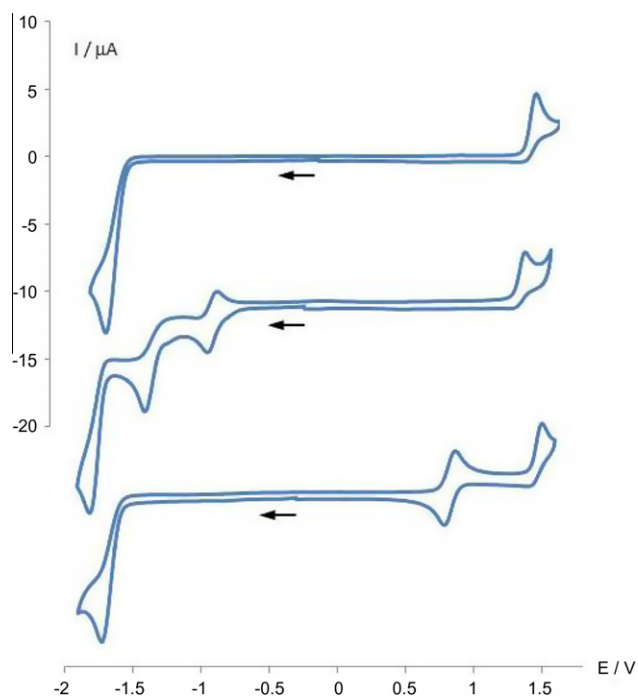


Fig. 8. Cyclic voltammograms for **2b** (upper), **2h** (middle) and **2f** (lower) at 100 mV s^{-1} (1×10^{-3} M in CH_2Cl_2 solution, 0.1 M Bu_4NPF_6 , referenced with equimolar $[\text{Fc}^{+}/0]$).

decamethylferrocene ($\text{Fc}^{+}/0$) reference standard was used, under which conditions $E^\circ [\text{Fc}^{+}/0] = 0.55 \text{ V}$ [77].

All samples display an irreversible one-electron oxidation associated with the $\text{Re}^{\text{I}}/\text{Re}^{\text{II}}$ couple at +1.5 V. The reversibility of this was not improved with decrease in temperature or increase in scan rate and variations associated with the differing triazole ligand substituents are within or close to the experimental error. For this oxidation the decamethylferrocene chemical reference is non-innocent and gives rise to some cathodic current on the reverse sweep.

For the reduction chemistry two distinct behaviours are observed. The voltammograms of rhenium complexes without a ligand nitro substituent (**2a–2c**, **2e–g**) are characterized by an irreversible multi-electron ligand based reduction wave. This occurs at ca. -1.7 V and the reversibility does not improve with increased scan rate. Between the two extremes of phenyl and octyl substituent (**2e** and **2a**) there is an apparent shift in E_{pc} commensurate with the predicted electronic properties of the substituent. To wit, **2e** (phenyl) E_{pc} occurs at -1.66 V, **2a** (octyl) is shifted 80 mV cathodically to -1.74 V. However like E_{pa} for the $\text{Re}^{\text{I}}/\text{Re}^{\text{II}}$ couple, any variability in E_{pc} observed for the other substituted ligand complexes is within or close to the experimental measure-

ment error. The ferrocenyl substituted triazole complex **2f** displays the predicted reversible oxidation couple associated with the metallocene fragment at $E^\circ = 0.85 \text{ V}$. This is a slight anodic shift from the naked ligand **1f** ($E^\circ = 0.78 \text{ V}$), and a result in line with our previous study of Pd triazole derivatives [24]. The current measured for this process is the same as that for the Re oxidation and thus provides supporting evidence for its one-electron assignment.

The two nitro substituted compounds show quite different reduction chemistry. The first two cathodic features are likely associated with the nitrobenzyl (**2d**)/nitrophenyl (**2h**) moieties and consist of a reversible one-electron reduction to a stable radical anion, followed by irreversible multi-electron processes. This behaviour closely resembles that previously reported for nitrobenzene [78,79]. The triazole reduction process for **2d** falls outside the scanned potential range.

The electrochemical data provide an indication of the energies of the redox active MOs such as the HOMO and LUMO. There is a substantial amount of literature that relates the energy separation observed between oxidation and reduction potentials with the observed optical transitions [80–82]. This correlation is particularly successful for MLCT transitions of metal polypyridyl complexes [83]. The comparison between the observed MLCT transitions and electrochemistry are consistent with this correlation, in that they show a separation between oxidation and reduction of approximately 3.2 eV which corresponds to a transition energy of 390 nm. This is slightly lower than observed (333 nm) but, importantly, is unchanged through the series. The exception is for complexes with the nitro-substituted ligands – the lack of correlation in these two cases is consistent with a redox orbital for the reduction that is unconnected to the acceptor MO in the lowest energy optical transition – that is a redox MO on the nitrobenzene unit. Analysis of the DFT data shows that for **2d** and **2h** the LUMO is in fact nitrobenzene based and furthermore the TD-DFT calculations show that the lowest energy transition of **2d** contains no LUMO character and in the calculation of **2h** the LUMO has a minor contribution to the calculated lowest energy transition. This latter point is consistent with the resonance Raman data of **2h** that reveals an enhancement of the nitro vibration indicating that the nitrobenzene group has some role in the electronic transition at 350 nm. As noted previously DFT calculations overestimate the level of conjugation in π -systems [66].

3. Conclusion

A family of electronically tuned *fac*- $\text{Re}^{\text{I}}(\text{CO})_3\text{Cl}$ pyridyl-1,2,3-triazole complexes have been synthesized in good to excellent yields by refluxing methanol solutions of $[\text{Re}(\text{CO})_5\text{Cl}]$ and the substituted 2-(1-R-1H-1,2,3-triazol-4-yl)pyridine ligands. The resulting rhenium(I) complexes were characterized by elemental analysis, HR-ESMS, IR, ^1H and ^{13}C NMR and in one case the molecular structure was confirmed by X-ray crystallography. A systematic study of the electronic structure of this family of *fac*-[(pytri-R) $\text{Re}(\text{CO})_3\text{Cl}$] complexes demonstrated that the MLCT transition energy, emission maxima and the electrochemical oxidation and reduction processes are all essentially unaffected by the electronic nature of the R substituent on the 2-(1-R-1H-1,2,3-triazol-4-yl)pyridine ligand. This indicates that the 1,2,3-triazole unit acts as an electronic insulator. The emission lifetimes of the complexes are dependent on the nature of the 1,2,3-triazole substituent, with the conjugated complexes displaying longer lifetimes than the non-conjugated ones. The shorter lifetime for complexes with non-conjugated ligands is attributed to the “free-rotor” effect which allows molecules to relax through non-radiative pathways. The electronic insulation of the triazole is illustrated by the resonance Raman

spectroscopy which shows near identical spectral signatures for the non-conjugated systems. This indicates that the resonant chromophore is unchanged by substitution. For the conjugated systems there are small changes with substitution reflecting modest perturbation of the chromophore. The 1,2,3-triazole unit offers a substitution platform that will not contaminate the electronic structure of the unsubstituted system. This property could be useful in the development of luminescent devices or bioprobes where the solubility of the “click” metal complexes could be rapidly tuned through substitution at the N1 nitrogen without affecting the intrinsic photophysical properties of the complexes.

Acknowledgements

This work was supported by the Department of Chemistry, University of Otago. C.J.M. thanks the New Economy Research Fund (Grant No. UOO-X0808) for financial support for this work.

Appendix A. Supplementary data

CCDC 872674 contains the supplementary crystallographic data for this paper. These data can be obtained free of charge via <http://www.ccdc.cam.ac.uk/conts/retrieving.html>, or from the Cambridge Crystallographic Data Centre, 12 Union Road, Cambridge CB2 1EZ, UK; fax: (+44) 1223-336-033; or e-mail: deposit@ccdc.cam.ac.uk. Supplementary data associated with this article can be found, in the online version, at <http://dx.doi.org/10.1016/j.poly.2012.05.003>.

References

- [1] Y. Kunitobu, K. Takai, *Chem. Rev.* 111 (2011) 1938.
- [2] Y. Kunitobu, A. Kawata, S.S. Yudha, H. Takata, M. Nishi, K. Takai, *Pure Appl. Chem.* 82 (2010) 1491.
- [3] H. Takeda, K. Koike, T. Morimoto, H. Inumaru, O. Ishitani, *Adv. Inorg. Chem.* 63 (2011) 137.
- [4] A. Coleman, C. Brennan, J.G. Vos, M.T. Pryce, *Coord. Chem. Rev.* 252 (2008) 2585.
- [5] R. Kirgan, B. Sullivan, D. Rillema, in: V. Balzani, S. Campagna (Eds.), *Topics in Current Chemistry*, vol. 281, Springer, Berlin/Heidelberg, 2007, p. 45.
- [6] H. Takeda, O. Ishitani, *Coord. Chem. Rev.* 254 (2010) 346.
- [7] A. Kumar, S.-S. Sun, A. Lees, in: A.J. Lees (Ed.), *Topics in Organometallic Chemistry*, vol. 29, Springer, Berlin/Heidelberg, 2010, p. 37.
- [8] A. Kumar, S.-S. Sun, A.J. Lees, *Coord. Chem. Rev.* 252 (2008) 922.
- [9] K.K.-W. Lo, K.Y. Zhang, S.P.-Y. Li, *Eur. J. Inorg. Chem.* 2011 (2011) 3551.
- [10] K. Lo, in: A.J. Lees (Ed.), *Topics in Organometallic Chemistry*, vol. 29, Springer, Berlin/Heidelberg, 2010, p. 73.
- [11] H. Struthers, T.L. Mindt, R. Schibli, *Dalton Trans.* 39 (2010) 675.
- [12] J.D. Crowley, A.-L. Lee, K.J. Kilpin, *Aust. J. Chem.* 64 (2011) 1118.
- [13] J. Crowley, D. McMorrán, *Topics in Heterocyclic Chemistry*, Springer, Berlin/Heidelberg, 2012, http://dx.doi.org/10.1007/7081_2011_67.
- [14] V.V. Rostovtsev, L.G. Green, V.V. Fokin, K.B. Sharpless, *Angew. Chem., Int. Ed.* 41 (2002) 2596.
- [15] P. Wu, V.V. Fokin, *Aldrichim. Acta* 40 (2007) 7.
- [16] J.E. Hein, V.V. Fokin, *Chem. Soc. Rev.* 39 (2010) 1302.
- [17] M. Meldal, C.W. Tornøe, *Chem. Rev.* 108 (2008) 2952.
- [18] C.W. Tornøe, C. Christensen, M. Meldal, *J. Org. Chem.* 67 (2002) 3057.
- [19] J.D. Crowley, P.H. Bandeen, L.R. Hanton, *Polyhedron* 29 (2010) 70.
- [20] J.D. Crowley, P.H. Bandeen, *Dalton Trans.* 39 (2010) 612.
- [21] O. Fleischel, N. Wu, A. Petitjean, *Chem. Commun.* 46 (2010) 8454.
- [22] L. Garcia, S.P. Maisonneuve, J. Xie, R.G. Guillot, P. Dorlet, E. Rivière, M. Desmadril, F.O. Lambert, C. Policar, *Inorg. Chem.* 49 (2010) 7282.
- [23] P.M. Guha, H. Phan, J.S. Kinyon, W.S. Brotherton, K. Sreenath, J.T. Simmons, Z. Wang, R.J. Clark, N.S. Dalal, M. Shatruck, L. Zhu, *Inorg. Chem.* 51 (2012) 3465.
- [24] K.J. Kilpin, E.L. Gavey, C.J. McAdam, C.B. Anderson, S.J. Lind, C.C. Keep, K.C. Gordon, J.D. Crowley, *Inorg. Chem.* 50 (2011) 6334.
- [25] K.J. Kilpin, J.D. Crowley, *Polyhedron* 29 (2010) 3111.
- [26] D. Schweinfurth, S. Strobel, B. Sarkar, *Inorg. Chim. Acta* 374 (2011) 253.
- [27] D. Schweinfurth, R. Pattacini, S. Strobel, B. Sarkar, *Dalton Trans.* (2009) 9291.
- [28] T.S. Romero, R.L.A. Orenes, A. Espinosa, A. Tarraga, P. Molina, *Inorg. Chem.* 50 (2011) 8214.
- [29] A.M. Najar, I.S. Tidmarsh, M.D. Ward, *CrystEngComm* 12 (2010) 3642.
- [30] C. Richardson, C.M. Fitchett, F.R. Keene, P.J. Steel, *Dalton Trans.* (2008) 2534.
- [31] J.T. Fletcher, B.J. Bumgarner, N.D. Engels, D.A. Skoglund, *Organometallics* 27 (2008) 5430.
- [32] B. Happ, C. Friebe, A. Winter, M.D. Hager, R. Hoogenboom, U.S. Schubert, *Chem. Asian J.* 4 (2009) 154.
- [33] C. Zhang, X. Shen, R. Sakai, M. Gottschaldt, U.S. Schubert, S. Hirohara, M. Tanihara, S. Yano, M. Obata, N. Xiao, T. Satoh, T. Kakuchi, *J. Polym. Sci., Part A* 49 (2011) 746.
- [34] M. Felici, P. Contreras-Carballada, Y. Vida, J.M.M. Smits, R.J.M. Nolte, L. De Cola, R.M. Williams, M.C. Feiters, *Chem. Eur. J.* 15 (2009) 13124.
- [35] D. Sykes, M.D. Ward, *Chem. Commun.* 47 (2011) 2279.
- [36] M. Juricek, M. Felici, P. Contreras-Carballada, J. Lauko, S.R. Bou, P.H.J. Kouwer, A.M. Brouwer, A.E. Rowan, *J. Mater. Chem.* 21 (2011) 2104.
- [37] S. Liu, P. Müller, M.K. Takase, T.M. Swager, *Inorg. Chem.* 50 (2011) 7598.
- [38] M. Mydlak, C. Bizzarri, D. Hartmann, W. Sarfert, G. Schmid, C.L. De, *Adv. Funct. Mater.* 20 (2010) 1812.
- [39] M. Obata, A. Kitamura, A. Mori, C. Kameyama, J.A. Czaplewski, R. Tanaka, I. Kinoshita, T. Kusumoto, H. Hashimoto, M. Harada, Y. Mikata, T. Funabiki, S. Yano, *Dalton Trans.* (2008) 3292.
- [40] I. Stengel, A. Mishra, N. Pootrakulchote, S.-J. Moon, S.M. Zakeeruddin, M. Graetzel, P. Baeuerle, *J. Mater. Chem.* 21 (2011) 3726.
- [41] M. Grätzel, *J. Photochem. Photobiol., C* 4 (2003) 145.
- [42] B. Happ, D. Escudero, M.D. Hager, C. Friebe, A. Winter, H. Gørls, E. Altuntas, L. Gonzalez, U.S. Schubert, *J. Org. Chem.* 75 (2010) 4025.
- [43] A. Mattiuzzi, I. Jabin, C. Moucheron, M.A. Kirsch-De, *Dalton Trans.* 40 (2011) 7395.
- [44] D. Schweinfurth, K.I. Hardcastle, U.H.F. Bunz, *Chem. Commun.* (2008) 2203.
- [45] A. Boulay, A. Seridi, C. Zedde, S. Ladeira, C. Picard, L. Maron, E. Benoist, *Eur. J. Inorg. Chem.* (2010) 5058.
- [46] A. Seridi, M. Wolff, A. Boulay, N. Saffon, Y. Coulais, C. Picard, B. Machura, E. Benoist, *Inorg. Chem. Commun.* 14 (2011) 238.
- [47] A.K. Feldman, B. Colasson, V.V. Fokin, *Org. Lett.* 6 (2004) 3897.
- [48] J. Andersen, S. Bolvig, X. Liang, *Synlett* (2005) 2941.
- [49] J. Andersen, U. Madsen, F. Bjorkling, X. Liang, *Synlett* (2005) 2209.
- [50] K.D. Grimes, A. Gupta, C.C. Aldrich, *Synthesis* (2010) 1441.
- [51] C.-Z. Tao, X. Cui, J. Li, A.-X. Liu, L. Liu, Q.-X. Guo, *Tetrahedron Lett.* 48 (2007) 3525.
- [52] V.O. Rodionov, S.I. Presolski, D. Díaz Díaz, V.V. Fokin, M.G. Finn, *J. Am. Chem. Soc.* 129 (2007) 12705.
- [53] R. Horvath, K.C. Gordon, *Inorg. Chim. Acta* 374 (2011) 10.
- [54] M.G. Fraser, C.A. Clark, R. Horvath, S.J. Lind, A.G. Blackman, X.Z. Sun, M.W. George, K.C. Gordon, *Inorg. Chem.* 50 (2011) 6093.
- [55] K.J. Kilpin, R. Horvath, G.B. Jameson, S.G. Telfer, K.C. Gordon, J.D. Crowley, *Organometallics* 29 (2010) 6186.
- [56] D.M. Cleland, G. Irwin, P. Wagner, D.L. Officer, K.C. Gordon, *Chem. Eur. J.* 15 (2009) 3682.
- [57] N.J. Lundin, P.J. Walsh, S.L. Howell, A.G. Blackman, K.C. Gordon, *Chem. Eur. J.* 14 (2008) 11573.
- [58] M.R. Waterland, S.L. Howell, K.C. Gordon, *J. Phys. Chem. A* 111 (2007) 4604.
- [59] S.L. Howell, K.C. Gordon, M.R. Waterland, K.H. Leung, D.L. Phillips, *J. Phys. Chem. A* 110 (2006) 11194.
- [60] N.J. Lundin, P.J. Walsh, S.L. Howell, J.J. McGarvey, A.G. Blackman, K.C. Gordon, *Inorg. Chem.* 44 (2005) 3551.
- [61] S.L. Howell, S.M. Scott, A.H. Flood, K.C. Gordon, *J. Phys. Chem. A* 109 (2005) 3745.
- [62] S.L. Howell, K.C. Gordon, J.J. McGarvey, *J. Phys. Chem. A* 109 (2005) 2948.
- [63] S.L. Howell, B.J. Matthewson, M.I.J. Polson, A.K. Burrell, K.C. Gordon, *Inorg. Chem.* 43 (2004) 2876.
- [64] S.L. Howell, K.C. Gordon, *J. Phys. Chem. A* 108 (2004) 2536.
- [65] B.J. Matthewson, A. Flood, M.I.J. Polson, C. Armstrong, D.L. Phillips, K.C. Gordon, *Bull. Chem. Soc. Jpn.* 75 (2002) 933.
- [66] T.M. Clarke, K.C. Gordon, D.L. Officer, S.B. Hall, G.E. Collis, A.K. Burrell, *J. Phys. Chem. A* 107 (2003) 11505.
- [67] T.M. Clarke, K.C. Gordon, D.L. Officer, D.K. Grant, *J. Phys. Chem. A* 109 (2005) 1961.
- [68] A.Y. Hirakawa, M. Tsuboi, *Science* 188 (1975) 359.
- [69] R.J.H. Clark, T.J. Dines, *Angew. Chem., Int. Ed.* 98 (1986) 131.
- [70] A. Flood, R.B. Girling, K.C. Gordon, R.E. Hester, J.N. Moore, M.I.J. Polson, *J. Raman Spectrosc.* 33 (2002) 434.
- [71] M.G. Fraser, A.G. Blackman, G.I.S. Irwin, C.P. Easton, K.C. Gordon, *Inorg. Chem.* 49 (2011) 5180.
- [72] M.R. Waterland, K.C. Gordon, *J. Raman Spectrosc.* 31 (2000) 243.
- [73] M.R. Waterland, K.C. Gordon, J.J. McGarvey, P.M. Jayaweera, *J. Chem. Soc., Dalton Trans.* (1998) 609.
- [74] N.J. Turro, V. Ramamurthy, J.C. Scaiano, *Modern Molecular Photochemistry of Organic Molecules*, University Science Books, Sausalito, California, 2010.
- [75] G.J. Stor, F. Hartl, J.W.M. van Outersterp, D.J. Stufkens, *Organometallics* 14 (1995) 1115.
- [76] S. Roy, C.P. Kubiak, *Dalton Trans.* 39 (2010) 10937.
- [77] F. Barriere, W.E. Geiger, *J. Am. Chem. Soc.* 128 (2006) 3980.
- [78] D.S. Silvester, A.J. Wain, L. Aldous, C. Hardacre, R.G. Compton, *J. Electroanal. Chem.* 596 (2006) 131.
- [79] W.H. Smith, A.J. Bard, *J. Am. Chem. Soc.* 97 (1975) 5203.
- [80] S. Campagna, F. Puntoriero, F. Nastasi, G. Bergamini, V. Balzani, in: V.C.S. Balzani (Ed.), *Photochemistry and Photophysics of Coordination Compounds I*, *Topics in Current Chemistry*, vol. 280, 2007, p. 117.
- [81] A. Juris, S. Campagna, I. Bidd, J.M. Lehn, R. Ziessel, *Inorg. Chem.* 27 (1988) 4007.
- [82] J. Sherborne, S.M. Scott, K.C. Gordon, *Inorg. Chim. Acta* 260 (1997) 199.
- [83] A. Vlcek Jr., S. Zalis, *Coord. Chem. Rev.* 251 (2007) 258.